(Received 13 September 2023, Accepted 1 March 2024, Scheduled 21 March 2024)

Noncontact Voltage Measurement System for Low-Voltage Power Line

Huafeng Su[1,*], Haojun Li[1], Weihao Liang[1], Chaolan Shen[2], and Zheng Xu[2]

[1] *Dongguan Power Supply Bureau of Guangdong Power Grid Co., LTD, Dongguan 523120, China*
[2] *School of Electrical Engineering, Chongqing University, Chongqing 400044, China*

ABSTRACT: As one of the most basic electric quantities in a power system, voltage plays an important role in many fields such as condition monitoring and fault diagnosis. The construction and development of the smart grid cannot be separated from the reform and progress of the advanced sensing and measurement technology. Noncontact voltage measurement technology, as one of the important technologies, has many advantages such as no electrical contact, low insulation requirements, easy installation, and great potential in improving the panoramic perception ability of the power system. In this paper, a noncontact measurement method of the power line voltage based on capacitive coupling principle is proposed, which realizes the reliable measurement of the line voltage waveform. First, the principle of the noncontact voltage measurement method is introduced, which mainly includes self-calibration and online measurement of the sensor. The high-frequency voltage signal is injected into the capacitive coupling network of the sensor to implement the self-calibration of the sensor. Then, the digital integration method is used to integrate the output signal of the sensor to measure the line voltage waveform. Second, the noncontact voltage sensor prototype and signal processing circuit are designed. Finally, the test platform of the line voltage measurement is built, and the measurement test of 220 V/50 Hz line voltage waveform is carried out. The test results show the relative amplitude error of the voltage measured by the sensor is less than 2.5%, the maximum phase error less than 2° at 50 Hz, and the linearity better than 0.5%. The frequency response experiment shows that the system has almost constant gain in the frequency range of 50–1800 Hz, and the phase error reaches a maximum of 2.8° at a frequency of 1800 Hz.

1. INTRODUCTION

The operation, monitoring, and maintenance of the smart power grid are inseparable from the accurate, rapid acquisition of various physical quantity information, including electricity volume (voltage and current). With the development of smart power grid, higher requirements are proposed for the power system sensor and measurement technology. The research and practice of smart power grid show advanced sensing, and measurement technology is an essential element of the smart power grid. At the same time, as the scale of power grid continues to expand, many distributed energy and power electronic devices have been introduced, in urgent need of advanced sensing and measurement technology to ensure the safety and reliability of power grid under complex operating conditions.

As one of the most basic electric quantities in the power system, voltage plays a crucial role in many aspects, such as electric energy measurement, relay protection and control, and online overvoltage monitoring. At present, in the power system, voltage measuring devices mainly include electromagnetic voltage transformer, capacitive voltage transformer, and optical voltage sensor. The electromagnetic voltage transformer and capacitive voltage transformer must be electrically connected to the line being measured. Therefore, the installation, calibration, and maintenance of such measuring devices must be carried out in case of power failure, which requires a large amount of manpower, financial, and material resources. At the same time, this kind of device is bulky, mainly made of ferromagnetic material, has inconvenient installation, and prone to the risk of core saturation and ferromagnetic resonance. Although optical voltage sensor can measure the line voltage by measuring the electric field, the stability of the optical device is greatly affected by temperature, humidity, and other factors. However, with the development of optical phase detection technology, the measurement accuracy of optical voltage sensors has been significantly improved. However, optical sensors require optical emission devices and optical signal processing devices, resulting in higher costs for sensors. The principle of the noncontact voltage measurement with thermoelastic effect is that the material undergoes elastic deformation when being heated. The electrode plate of the capacitor made of this material vibrates to produce changing capacitance. A current proportional to the potential of the conductor being measured flows through the changing capacitance. Voltage measurement is achieved by processing the current signal [1]. However, the response speed of the thermoelastic effect driven structure is related to the thermal expansion time constant of the material and is easily affected by the ambient temperature. Changes in external ambient temperature can seriously interfere with measurement accuracy. This method is also called vibration capacitance modulation principle. The method of driving capacitor electrode plate vibration can be based on magnetostriction effect, acoustic emission, ultrasound, and others. These methods are more

* Corresponding author: Huafeng Su (suhf2023@163.com).

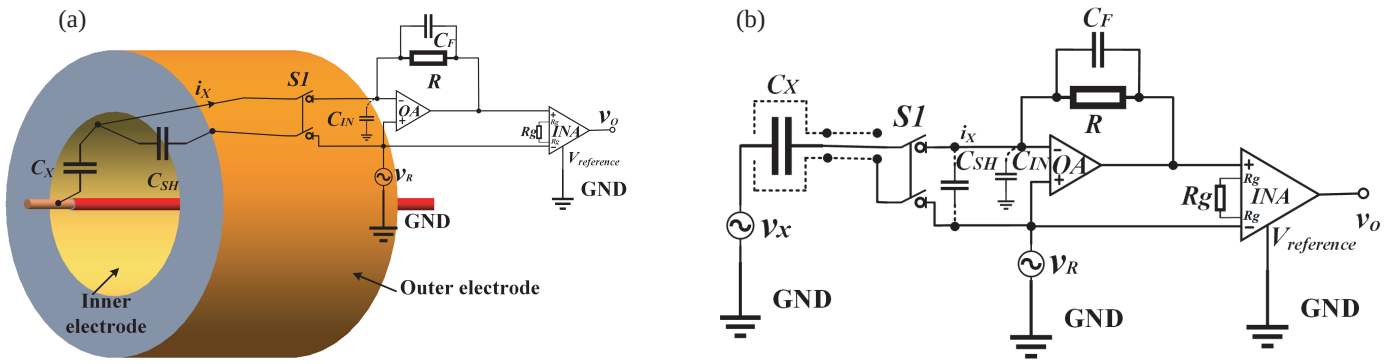

FIGURE 1. (a) 3D structure diagram of voltage sensor. (b) Equivalent circuit diagram of signal processing circuit.

suitable for DC potential measurement, and the changing capacitance requires complex hardware driving devices, which increases the cost and power consumption of the system [2]. Thus, the research of a new type of voltage sensor to implement the noncontact, reliable measurement of line voltage is the future focus of sensor measurement technology.

Zisman proposed a noncontact measurement method based on electrostatic potential for the first time [3]. In this method, the author placed a vibrating plate near the measured potential to form a time-varying capacitor and determined the measured potential by adjusting the voltage of the plate and monitoring the current flowing through the plate. Reference [4] proposed a method to improve the bandwidth of the measurement potential of the sensor by integrating the current flowing through the plate.

Noncontact voltage measurement technology without electrical contact is adopted to measure the line voltage, which greatly improves the safety of operation and eliminates the need to peel off the insulation layer of the wire, thus greatly reducing the risk of electric shock caused by bare wire. At present, many researchers have studied voltage root mean square (RMS) measurement [5–10], and mature products already exist in the market [11]. Methods for measuring the voltage of transmission lines and corresponding contactless voltage sensors have also been proposed [12, 13]. In [14], a differential capacitive sensor for measuring single-phase enclosed two-wire residential entrance lines has been designed, and the sensor is calibrated by a multimeter to achieve accurate voltage measurement (so called Semi-Contactless). The same measurement principle appears in [15]. A new voltage sensor structure is designed to solve the issue that the theoretical capacitance of the sensor is smaller than the actual one due to the edge effect, and ceramic capacitors are connected in parallel between two electrode plates of the sensor to improve the low-frequency performance of the sensor. A voltage probe in [16] is proposed for voltage measurement of an insulated cable/wire, in which a reference signal with high frequency is applied. Finally, the voltage amplitude is calculated on the basis of measured quantities.

However, few researchers have examined the measurement of the voltage instantaneous waveform. Based on the principle of capacitive coupling, the noncontact voltage measurement technology combined with analog circuit and digital signal processing (DSP) technology to measure the voltage waveform of power lines has been verified [17]. Reference [18] analyzed the noise in noncontact voltage measurement. However, practical experiments revealed a large high-frequency noise signal in the power line voltage measurement, which has a great negative effect on the measurement accuracy. Moreover, the calibration method proposed in [17] requires human intervention and is complicated in operation.

This paper presents a noncontact voltage measurement system for power line voltage measurement. The shortcoming of human intervention in the measurement in [17] is solved; the entire measurement is automatically implemented by the controller; and the method solves the problem that the high-frequency noise in the signal affects the measurement accuracy when the power line voltage is measured.

2. METHOD

2.1. Principle of Voltage Measurement

Figures 1(a) and (b) show the 3D structure diagram of the proposed voltage sensor and the equivalent circuit diagram of the signal processing circuit, respectively. Fig. 1(a) shows the voltage sensor composed of two electrodes, namely the inner electrode and outer electrode. The inner and outer electrodes are insulated by insulating materials. The outer electrode is grounded by a high-frequency signal v_R, and the inner electrode and outer electrode are connected to the input end of the transimpedance amplifier (TIA) through a coaxial cable. Because the frequency of v_R is much higher than the frequency of the power line voltage, the external electrode can be considered directly grounded to achieve electromagnetic shielding. In Fig. 1(b), R and C_F are the feedback resistance and compensation capacitor of the TIA, respectively. The role of C_F is to compensate TIA for its stable operation [19]. According to the principle of virtual short and virtual break of the operational amplifier, no current flowing through the mutual capacitance C_{SH} which is formed by the inner electrode and outer electrode. The inner and outer electrodes of the voltage sensor are connected to the inner core and the shielding layer of the coaxial cable, respectively, and parasitic capacitance between the two poles of the coaxial cable can remarkably increase C_{SH}. The measured conductor with voltage v_X penetrates through the voltage sensor as shown in

Fig. 1(a). Mutual capacitance C_X is formed between the inner electrode and measured conductor, and v_X in the measured conductor generates an alternating electric field in space. Thus, displacement current i_X flows through C_X, and the Laplace transform of the relationship between i_X and v_X is

$$I_X(s) = [V_X(s) - V_R(s)] \cdot s \cdot C_X \quad (1)$$

Figure 1(b) shows the equivalent circuit of the sensor and signal processing circuit. i_X is converted and amplified into the differential voltage signal through the TIA. The differential signal is then differentially amplified by the instrument amplifier (INA) and converted into a single-ended signal v_O, making it compatible with the single-ended input analog-to-digital converter (ADC). Resistor R_g is the meter amplifier gain-regulating resistor. $S1$ is a two-pole, single-throw analog switch that turns on and off automatically through a microcontroller unit (MCU) to control the self-calibration of sensor. The role of the switch is to eliminate human involvement during the measurement process. When $S1$ is closed, the circuit output is given by (2):

$$V_O(s) = [-I_X(s) + V_R(s) \cdot s \cdot C_{IN}] \cdot R \cdot G_{INA} \quad (2)$$

In the above equation, $I_X(s)$ is the current flowing through C_X, C_{IN} the parasitic capacitance generated by the wiring of the op amp and printed circuit board, and G_{INA} the gain of the instrument amplifier. Combining (1) and (2), if $V_R(s) = 0$, $sV_X(s)$ and $V_O(s)$ are proportional, and the scaling factor $G_X = R \cdot C_X \cdot G_{INA}$.

The application of high-frequency voltage signal v_R in signal processing circuit has two functions: First, it eliminates the error of voltage measurement caused by the parasitic capacitor C_{IN} and calibrates the system. Second, it is used to estimate scaling factor G_X. The compensation capacitor C_F only acts at high frequency and does not affect the system transfer function.

MCU is an important part of measurement system, which is responsible for DSP and control. MCU has three main functions. First, implement self-calibration of voltage sensors, measurement of unknown AC voltage waveforms and send the waveforms data to the upper computer for display. Second, MCU controls the opening and closing of switch $S1$, to achieve automatic switching between calibration and measurement modes. Last, MCU generates high-frequency voltage signal v_R using its built-in digital-to-analog converter (DAC) peripherals. When MCU is powered on, it automatically carries out the calibrations to calibrate the voltage sensor. After that, it automatically switches to the measurement mode, and the whole process is automatically completed through MCU.

2.2. Voltage Sensor Self-Calibration Method Based on High-Frequency Voltage Signal Injection

The voltage sensor self-calibration method based on high-frequency voltage signal injection can be divided into two steps, namely, offline calibration and online calibration. Offline calibration determines the additional output signal generated by the parasitic capacitor C_{IN}. Online calibration determines the scaling factor G_X, by penetrating the measured conductor with a voltage of v_X through the voltage sensor. First, MCU automatically performs offline calibration, and MCU control switch $S1$ is opened to remove the voltage sensor from the circuit (i.e., $C_X = 0$). v_X does not contribute to the output of INA, and the output is completely generated by v_R. Define $G_{IN} = C_{IN} \cdot R \cdot G_{INA}$, and the output signal amplitude V_{CR} is shown in (3):

$$V_{CR} = 2\pi f_R \cdot V_R \cdot C_{IN} \cdot R \cdot G_{INA} = 2\pi f_R \cdot V_R \cdot G_{IN}, \quad (3)$$

where V_R and f_R are the amplitude and frequency of v_R, respectively. V_{CR} is obtained by measurement, and the output signal generated by the parasitic capacitor C_{IN} is obtained through a single calibration.

Second, MCU automatically carries out online calibration. Switch $S1$ is closed, and the voltage sensor is connected to the circuit. The output of INA can be expressed as follows:

$$V_O(s) = -s \cdot G_X \cdot V_X(s) + s \cdot (G_X + G_{IN}) \cdot V_R(s) \quad (4)$$

The circuit output is generated by v_X and v_R. Because f_R is much higher than the frequency of v_X, the output signal generated by v_R can be simply extracted from the output signal through the frequency spectrum analysis. The amplitude of output generated by v_R is defined as V_{OR}, and V_{OR} is given by (5):

$$V_{OR} = 2\pi f_R \cdot V_R \cdot (G_X + G_{IN}) \quad (5)$$

Combining (3) and (5), we can estimate the value of C_X. Furthermore, $\hat{G}_X$ is the approximation of G_X and can be calculated by (6):

$$\hat{G}_X = \frac{\hat{V}_{OR} - \hat{V}_{CR}}{2\pi f_R \cdot V_R} \quad (6)$$

where $\hat{V}_{OR}$ and $\hat{V}_{CR}$ are obtained by measurement and represent the approximations of V_{OR} and V_{CR}. The system can implement the unknown voltage waveform measurement after the offline and online calibrations. To ensure that the estimated $\hat{G}_X$ can accurately restore v_X, v_X in (4) should not contain any components with the frequency equal to f_R. Otherwise, the scaling factor $\hat{G}_X$ estimated by the above method has a large deviation from the actual G_X. Therefore, the frequency of sinusoidal reference signal v_R must be carefully selected.

2.3. Online Voltage Measurement

During this step, the system can continuously measure the waveform of unknown voltage v_X. The specific operation of online voltage measurement is as follows: v_R is removed from the circuit, and the outer electrode of the voltage sensor is grounded (i.e., $V_R(s) = 0$). The output is completely generated by v_X and can be expressed as follows:

$$V_O(s) = -s \cdot G_X \cdot V_X(s) \quad (7)$$

$V_O(s)$ is digitally integrated and divided by the scale factor $-\hat{G}_X$, as shown in (8), to measure the voltage waveform v_X of the measured conductor:

$$\hat{V}_X(s) = -\frac{V_O(s)}{s \cdot \hat{G}_X} \quad (8)$$

The voltage waveform measured by the above method can retain the phase information of the waveform.

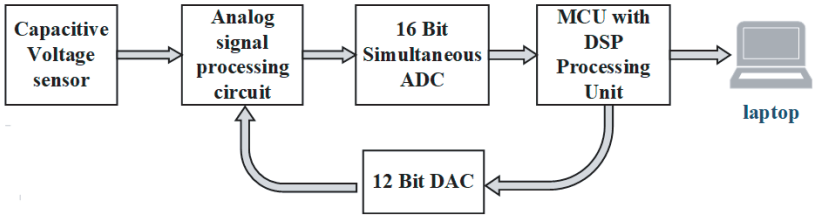

FIGURE 2. System overall structure diagram.

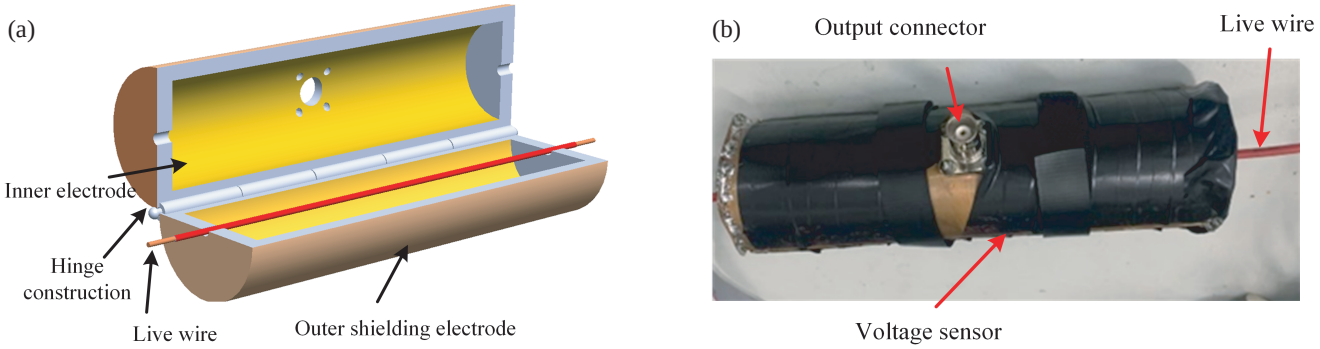

FIGURE 3. (a) Voltage sensor 3D view. (b) Physical diagram of voltage sensor.

3. SYSTEM IMPLEMENTATION

3.1. Hardware Design

The overall design diagram of the hardware circuit is shown in Fig. 2. The signal processing circuit receives the output signal of the voltage sensor and the high-frequency voltage signal generated by the 12-bit DAC module. Then, the output signal of the signal processing circuit is sampled by the 16-bit synchronous sampling module, and the collected digital signal is processed by MCU with DSP unit. Finally, The MCU utilizes the received data to restore the measured voltage waveforms and sends them to the laptop for display.

Figure 3 shows the voltage sensor consisting of two hinged semicylinders. This structure allows easy opening and closing of the sensor to place the measured conductor. The inner and outer surfaces of the sensor are wrapped with a layer of metal copper. The diameter of the inner surface of the cylinder is 30 mm, and the length is 120 mm. The inner copper skin constitutes the inner electrode. The diameter of the outer surface cylinder is 50 mm, and the length is 150 mm. The outer copper skin forms the outer shielding electrode. The outer shielding layer needs to wrap the inner electrode inside completely to improve the shielding effectiveness against external electromagnetic interference. The inner electrode and electromagnetic shielding shell are separated by a white resin material, and the two are insulated from each other.

Four threaded holes are on the voltage sensor. A Bayonet Nut Connector (BNC) female connector with flange is fixed on the voltage sensor by four M2.5 Phillips screws. The BNC female connector is connected to the span TIA with a coaxial cable that reduces interference introduced during signal transmission. The value of capacitance C_X can be approximated by (9) for estimating coaxial cylindrical capacitance:

$$C_X \approx \frac{2\pi\varepsilon_0 L}{\ln(\phi_E/\phi_C)} \tag{9}$$

where $\varepsilon_0 = 8.85$ pF/m in vacuum; L and ϕ_E are the length and diameter of the measured electrode, respectively; and ϕ_C is the conductor diameter. For the designed voltage sensor, $\phi_E = 30$ mm, $L = 120$ mm, and $\phi_C = 5.83$ mm (AWG3 wire). With the above parameters, C_X can be calculated to be equal to 4 pF using (9).

OAP320 (TI Company) is adopted as the TIA, which has ultralow input bias current and noise. The amplification factor of the TIA is adjusted by adjusting the feedback resistance R, which is set to 2 MΩ. Thus, if $C_X = 4$ pF, the maximum voltage $|V|_{MAX}$ that the system can measure is given by the following equation:

$$|V|_{MAX} \leq \frac{2.5}{2\pi f \cdot R \cdot C} \tag{10}$$

where f is the frequency of the measured voltage, and the measurement range can reach ±1000 V for the frequency of 50 Hz. INA128 produced by TI company is used as the instrument amplifier. By setting the resistance value of the gain resistor R_g to 50 kΩ, the gain of the instrument amplifier is 2. AD7606 synchronous sampling chip produced by ADI is used for synchronous acquisition of output signals of precision voltage sensor and designed voltage sensor. The chip has a resolution of 16 bits and a maximum sampling rate of 200 ksps.

3.2. Digital Signal Processing

1) MCU: MCU uses STM32F407VET6 from STMicroelectronics for control and digital signal processing, which is a

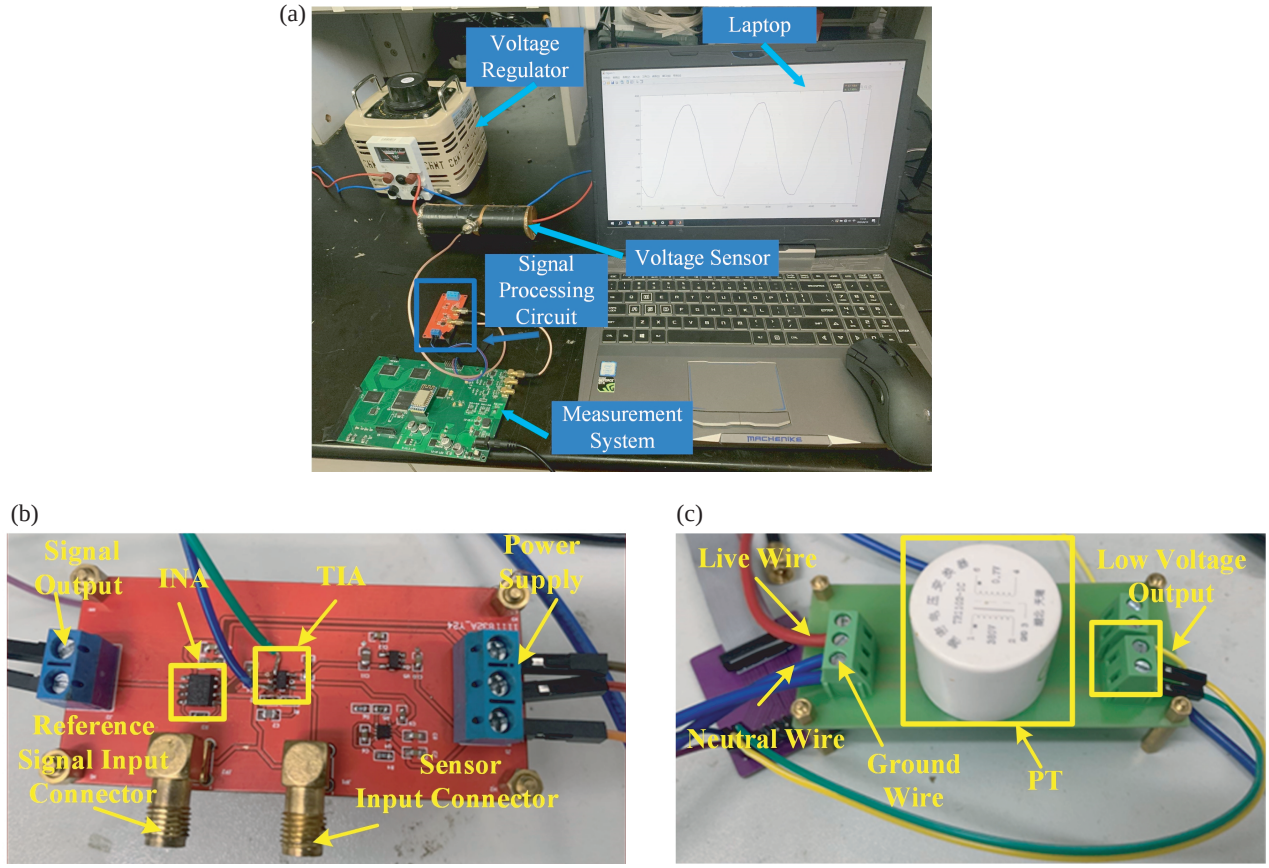

FIGURE 4. Experimental platform and measurement circuit. (a) Experimental platform. (b) Signal processing circuit. (c) Reference voltage measurement circuit.

high-performance microcontroller based on ARM Cortex-M4. MCU and laptop are connected via a serial port, and the laptop is used to store and display the data received. The high-frequency voltage signal v_R is generated by the MCU's built-in 12-bit DAC peripheral. The signal amplitude is 2 V, and the frequency is $f_R = 2.5$ kHz. The sampling frequency of ADC is $f_S = 100$ kHz, which has two advantages:

a) The sampling frequency is an integer multiple of f_S, which can prevent spectrum leakage during the spectrum analysis of the signal.
b) The higher sampling rate can solve the problem of baseline drift caused by frequency aliasing caused by the frequency analysis of signals and the digital integration of signals caused by high-frequency components in the signals.

2) Sinusoidal Signal Estimation: First, for the sinusoidal signal V_{OC} amplitude obtained in offline mode, fast Fourier transform (FFT) on the output signal is performed in offline mode to calculate the signal spectrum. At this time, the output signal only includes the component with frequency f_S. The signal amplitude with frequency f_S from the spectrum is found to obtain the estimated $\hat{V}_{CR}$. Second, the V_{OR} signal is extracted from the output signal v_O of online calibration mode. Because the signal includes multiple frequency components, incoherent noise in the signal is removed by the coherent averaging method first [20]. The weighted average signal segments are transformed by FFT to find the signal amplitude with a frequency of f_R.

3) Digital Filter and Integrator: Due to the influence of the mismatch voltage of operational amplifiers, low-frequency components are unrelated to useful signals in the output signal, and such low-frequency components cause problems in the integration of signals. Digital high-pass filter is a feasible solution to remove the low-frequency components in the signal. The high-pass filter uses a second-order finite impulse response filter. The cut-off frequency of the filter is 0.5 Hz. The high-pass filter output is the input to the digital integrator, which uses the Simpson integral method (Newton-Cotes coefficient: 1/6, 4/6, 1/6). The output of the integrator is calculated by (10):

$$y(n) = y(n-1) + \frac{[v_O(n-1) + 2 \times (v_O(n) + v_O(n-1)) + v_O(n)]}{(6 \times f_S)} \quad (11)$$

where n represents the discrete time point, and $y(n)$ represents the signal value of the integrator's output at discrete time n.

4. EXPERIMENT RESEARCH

The MCU system integrates MCU, ADC, and Wi-Fi module, which is shown in Fig. 4(a) and is used to generate the high-frequency signal and process digital signals to achieve sensor

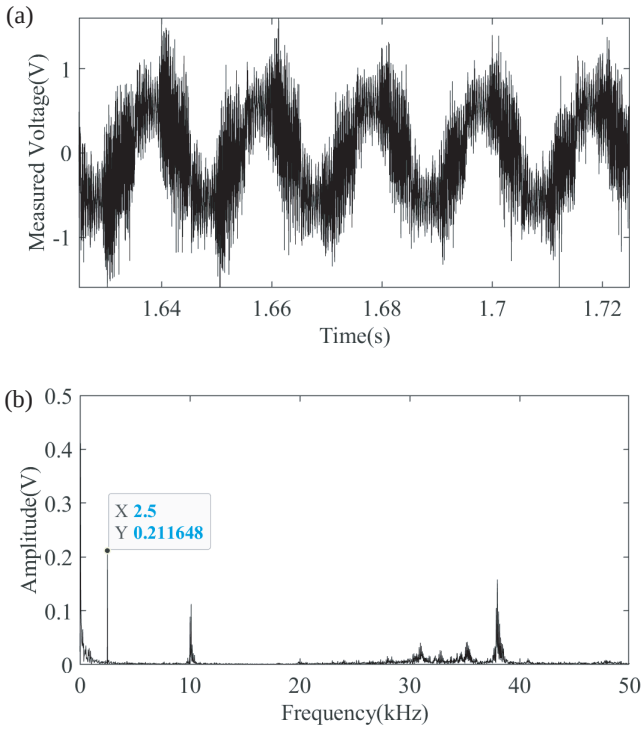

FIGURE 5. (a) Online calibration output signal. (b) Signal spectrum.

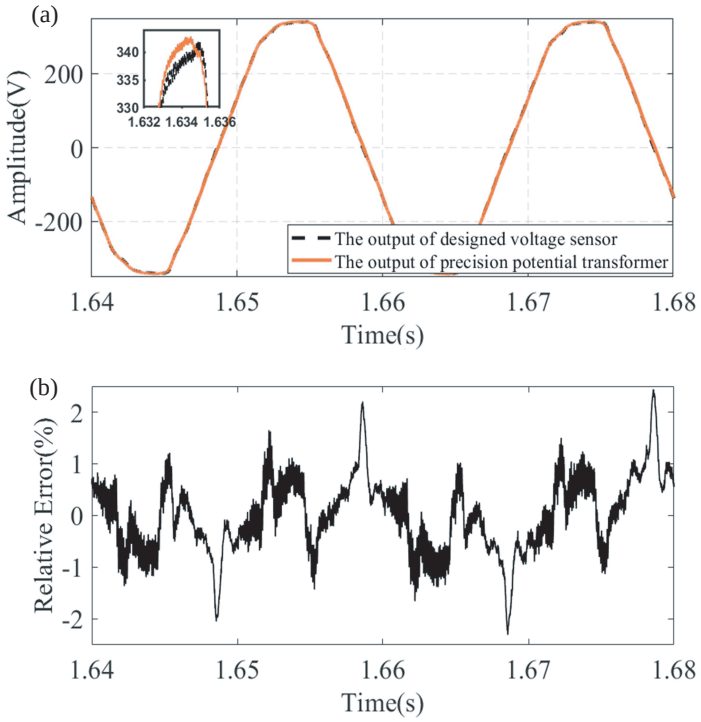

FIGURE 6. Power line voltage waveforms. (a) The output of designed voltage sensor and precision potential transformer. (b) Instantaneous relative error curve.

calibration and NC voltage measurement. The induced current of the voltage probe is converted into a voltage signal by the signal processing circuit and sent to the MCU system. The system measures the reference voltage by the precision voltage transformer (PT) TR1102-C. The measured voltage signal is sent to the laptop through wireless Wi-Fi for display.

4.1. Sensor Calibration Experiment

Voltage v_R with $f_R = 2.5$ kHz and $V_R = 1$ V was applied into the signal processing circuit to calibrate the measuring system. The output signal of offline calibration is a single frequency sinusoidal signal, and the amplitude of the output sinusoidal signal reflects the value of C_{IN}. During the online calibration, the output and its spectrum of the INA are shown in Figs. 5(a) and (b). In Fig. 5(a), The vertical axis represents the signal amplitude; the unit is V; the horizontal axis represents the time; the unit is ms. In Fig. 5(b), the horizontal axis is the signal amplitude; the unit is V; the vertical axis is the frequency; the unit is kHz. Fig. 5(b) shows that the amplitude of the component with frequency 2.5 kHz is about 0.211 V. The scale factor can be calculated from the above information to be equal to 5.4×10^{-6}.

4.2. Voltage Measurement for Power Line

The designed voltage sensor is used to measure the power line voltage waveform of 220 V/50 Hz. To evaluate the measurement accuracy of the system, the reference voltage waveform of the power line is obtained by the PT. The ratio and accuracy of the PT are 380 : 0.7 and 0.2%, respectively, and the phase shift of the PT can be ignored. The measured line voltage can be restored by multiplying the low voltage output of the precision voltage sensor with a fixed gain. The output signals of the PT and voltage sensor are synchronously sampled by AD7606 to evaluate the accuracy of sensor phase measurement. The AD7606 from ADI can implement 8-channel synchronous sampling. The measured conductor of voltage is the live wire leading from a live plug bar. The measured voltage waveform is shown in Fig. 6. The dotted orange line is the voltage waveform measured by the voltage sensor, and the solid black line is the voltage waveform measured by PT. The phase error between the two waveforms is less than 2°, the absolute error of waveform peak less than 5 V, and the maximum relative error less than 2.5%.

4.3. Linearity

To evaluate the linearity of the voltage sensor, a voltage regulator is used to generate variable voltage. The input of the regulator is 220 V/50 Hz main voltage, and the RMS range of the regulator output is 0–250 V. Five voltages with different amplitudes are measured, and the voltage RMSs are 58.2, 84.9, 114.3, 170.7, and 248.4 V. The designed voltage sensor is used to measure the voltage, and the reference voltage is obtained by PT. The experiment results are given by the biaxial coordinate system in Fig. 7. The horizontal coordinate represents the voltage RMS measured by the PT as the reference value; the left vertical axis represents the RMS measured by the voltage sensor; and the five voltage RMSs measured by the voltage sensor are used for linear fitting. The right axis represents the relative

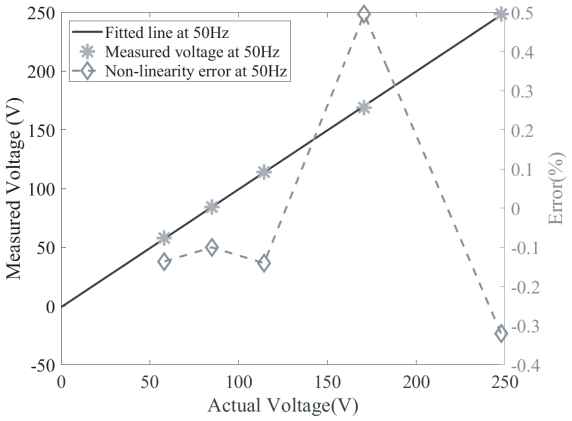

FIGURE 7. Linearity assessment of noncontact measurement at 50 Hz.

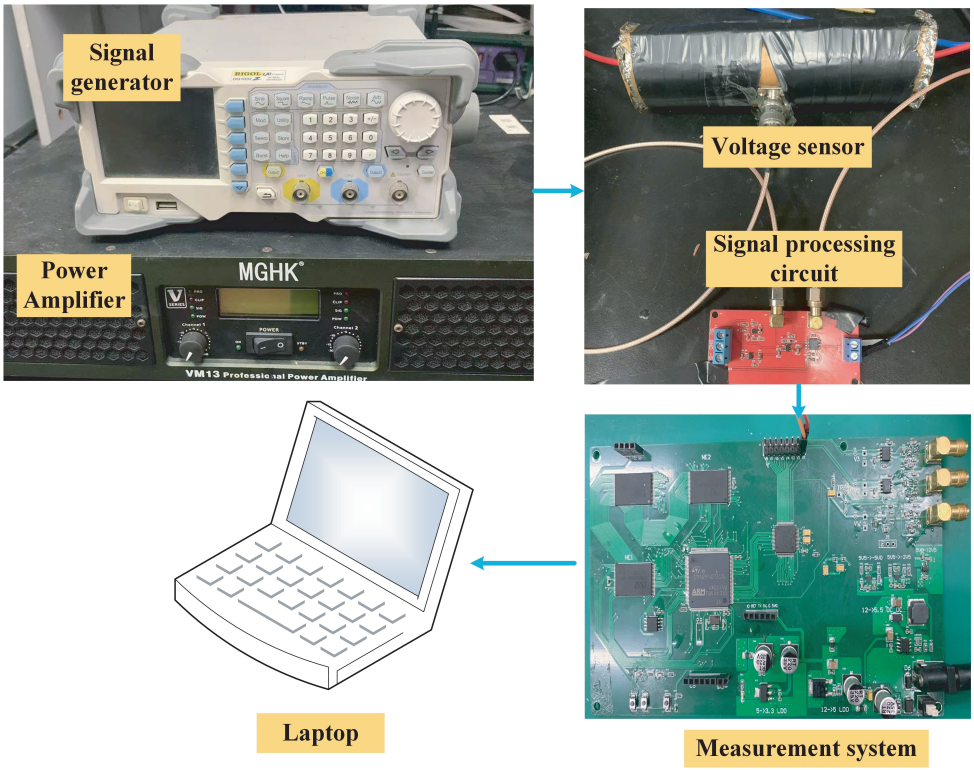

FIGURE 8. Frequency response experimental platform.

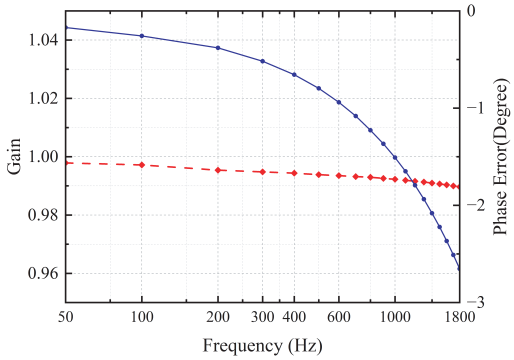

FIGURE 9. Frequency response of the voltage sensor.

error between the voltage measured by the voltage sensor and the fitting curve. The fitted curve is shown as the solid line in Fig. 7. The designed voltage sensor has good linearity for measuring RMS. The dashed line represents the curve connected by the relative measurement errors of the voltage sensor at five voltage measurement points. The relative measurement error of the voltage sensor is less than 0.5%.

4.4. Frequency Response

We conducted experiments to evaluate the frequency characteristics of the designed voltage sensor prototype. The frequency response characteristic experimental platform is shown in Fig. 8. The RIGOL DQ1032 signal generator generates a sine signal with a frequency range of 50–1800 Hz, which is amplified to 25 V by the power amplifier to drive the measured conductor. By measuring the unknown AC voltage waveform in the conductor using the designed voltage sensor, the reference voltage waveform through PT is obtained. The experimental results are shown in Fig. 9, in which the horizontal axis represents the frequency (Hz); the left vertical axis represents the gain; and the right vertical axis represents the phase error (°). The designed voltage sensor has almost constant gain coefficient in the frequency range of 50–1800 Hz, and the phase error is maximum at 1800 Hz about 2.8°.

5. CONCLUSION

This paper presents a noncontact voltage measurement method based on capacitive coupling principle, designs a noncontact voltage waveform measurement system suitable for low-voltage power line, and expounds the implementation of the system. A cylindrical descriptive voltage sensor prototype is designed for voltage measurement of power line. The openable structure of the voltage sensor makes the installation of the measured insulating conductor more convenient. A signal processing circuit is designed. The operational amplifier OPA320 with ultralow bias current is used as the TIA, and the low-noise instrument amplifier INA128 converts the differential voltage output of the TIA into the single-ended voltage signal compatible with the ADC. The processor used in the system is STM32F407VET6 (produced by ST microelectronics). The system can automatically achieve self-calibration of voltage sensor and AC voltage measurement. A laptop receives the data from the system for display.

The voltage waveform measurement experiment of noncontact 220 V/50 Hz main voltage is carried out. The experimental results show that the waveform measured by the designed voltage sensor is the same as that measured by the PT, and the phase error of the two waveforms is less than 2°. The relative error is less than 2.5%. The linearity of the noncontact measurement system for 50 Hz power line voltage RMS is verified. The variable voltage is obtained by a voltage regulator, and the experimental results show that the maximum nonlinear error of the system is less than 0.5%. The frequency response experiment shows that the system has good frequency characteristics; the system has almost constant gain in the frequency range of 50–1800 Hz; the phase error reaches a maximum of 2.8° at a frequency of 1800 Hz.

REFERENCES

[1] Chen, X., C. Peng, H. Tao, C. Ye, Q. Bai, S. Chen, and S. Xia, "Thermally driven micro-electrostatic fieldmeter," *Sensors and Actuators A: Physical*, Vol. 132, No. 2, 677–682, 2006.

[2] Wang, D., P. Li, and Y. Wen, "Design and modeling of magnetically driven electric-field sensor for non-contact DC voltage measurement in electric power systems," *Review of Scientific Instruments*, Vol. 87, No. 10, 105001, 2016.

[3] Zisman, W. A., "A new method of measuring contact potential differences in metals," *Review of Scientific Instruments*, Vol. 3, No. 7, 367–370, 1932.

[4] Vosteen, W. E., "A high speed electrostatic voltmeter technique," in *Conference Record of the 1988 IEEE Industry Applications Society Annual Meeting*, 1617–1619, Oct. 1988.

[5] Donnal, J. S. and S. B. Leeb, "Noncontact power meter," *IEEE Sensors Journal*, Vol. 15, No. 2, 1161–1169, 2015.

[6] Donnal, J. S., P. Lindahl, D. Lawrence, R. Zachar, and S. Leeb, "Untangling non-contact power monitoring puzzles," *IEEE Sensors Journal*, Vol. 17, No. 11, 3542–3550, 2017.

[7] Lindahl, P., G. Bredariol, J. Donnal, and S. Leeb, "Noncontact electrical system monitoring on a US Coast Guard cutter," *IEEE Instrumentation & Measurement Magazine*, Vol. 20, No. 4, 11–20, 2017.

[8] Shenil, P. S., R. Arjun, and B. George, "Feasibility study of a non-contact AC voltage measurement system," in *2015 IEEE International Instrumentation and Measurement Technology Conference (I2MTC) Proceedings*, 399–404, IEEE, May 2015.

[9] Shenil, P. S. and B. George, "An efficient digitizer for non-intrusive AC voltage measurement," in *2017 IEEE International Instrumentation and Measurement Technology Conference (I2MTC)*, 1–6, IEEE, May 2017.

[10] Shenil, P. S. and B. George, "Development of a nonintrusive true-RMS AC voltage measurement probe," *IEEE Transactions on Instrumentation and Measurement*, Vol. 68, No. 10, 3899–3906, 2019.

[11] Fluke Corporation, "Fluke T6 electrical testers with fieldsense technology," Accessed: Jun. 2019. [Online]. Available: [Online].https://www.fluke.com/esar/producto/comprobacionelectrica/comprobadores-basicos/fluke-t6-1000.

[12] Xiao, D., Y. Xie, Q. Ma, Q. Zheng, and Z. Zhang, "Non-contact voltage measurement of three-phase overhead transmission line based on electric field inverse calculation," *IET Generation, Transmission & Distribution*, Vol. 12, No. 12, 2952–2957, 2018.

[13] Chen, K.-L., Y. Guo, and X. Ma, "Contactless voltage sensor for overhead transmission lines," *IET Generation, Transmission & Distribution*, Vol. 12, No. 4, 957–966, 2018.

[14] Liu, X., W. He, P. Guo, Y. Yang, T. Guo, and Z. Xu, "Semi-contactless power measurement method for single-phase enclosed two-wire residential entrance lines," *IEEE Transactions on Instrumentation and Measurement*, Vol. 71, 1–16, 2022.

[15] Tan, X., W. Zhang, M. He, W. Li, G. Ao, and F. Zhou, "Non-contact adaptive voltage sensor based on electric field coupling principle," *Sensors*, Vol. 23, No. 19, 8316, 2023.

[16] Shenil, P. S. and B. George, "Nonintrusive AC voltage measurement unit utilizing the capacitive coupling to the power system ground," *IEEE Transactions on Instrumentation and Measurement*, Vol. 70, 1–8, 2020.

[17] Haberman, M. A. and E. M. Spinelli, "A noncontact voltage measurement system for power-line voltage waveforms," *IEEE*

Transactions on Instrumentation and Measurement, Vol. 69, No. 6, 2790–2797, 2020.

[18] Haberman, M. A. and E. M. Spinelli, "Noncontact AC voltage measurements: Error and noise analysis," *IEEE Transactions on Instrumentation and Measurement*, Vol. 67, No. 8, 1946–1953, 2018.

[19] Bhat, A., "Stabilize your transimpedance amplifier," *Maxim Integr.*, San Jose, CA, USA, 2012.

[20] Rompelman, O. and H. H. Ros, "Coherent averaging technique: A tutorial review part 1: Noise reduction and the equivalent filter," *Journal of Biomedical Engineering*, Vol. 8, No. 1, 24–29, 1986.